Journal of Biomechanics 47 (2014) 505–511

Contents lists available at ScienceDirect

Journal of Biomechanics

journal homepage: www.elsevier.com/locate/jbiomech
www.JBiomech.com

Hemodynamics in coronary arteries with overlapping stents

Farhad Rikhtegar [a], Christophe Wyss [b], Kathryn S. Stok [c], Dimos Poulikakos [a], Ralph Müller [c], Vartan Kurtcuoglu [a,d,*]

[a] Laboratory of Thermodynamics in Emerging Technologies, Department of Mechanical and Process Engineering, ETH Zurich, Zurich, Switzerland
[b] Clinic of Cardiology, University Hospital Zurich, Zurich, Switzerland
[c] Institute for Biomechanics, Department of Health Sciences and Technology, ETH Zurich, Zurich, Switzerland
[d] The Interface Group, Institute of Physiology, University of Zurich, Winterthurerstrasse 190, Y23 J8, 8057 Zurich, Switzerland

ARTICLE INFO

Article history:
Accepted 26 October 2013

Keywords:
Stent overlap
Thrombosis
Hemodynamics
Wall shear stress
Restenosis

ABSTRACT

Coronary artery stenosis is commonly treated by stent placement via percutaneous intervention, at times requiring multiple stents that may overlap. Stent overlap is associated with increased risk of adverse clinical outcome. While changes in local blood flow are suspected to play a role therein, hemodynamics in arteries with overlapping stents remain poorly understood. In this study we analyzed six cases of partially overlapping stents, placed ex vivo in porcine left coronary arteries and compared them to five cases with two non-overlapping stents. The stented vessel geometries were obtained by micro-computed tomography of corrosion casts. Flow and shear stress distribution were calculated using computational fluid dynamics. We observed a significant increase in the relative area exposed to low wall shear stress (WSS $<$ 0.5 Pa) in the overlapping stent segments compared both to areas without overlap in the same samples, as well as to non-overlapping stents. We further observed that the configuration of the overlapping stent struts relative to each other influenced the size of the low WSS area: positioning of the struts in the same axial location led to larger areas of low WSS compared to alternating struts. Our results indicate that the overlap geometry is by itself sufficient to cause unfavorable flow conditions that may worsen clinical outcome. While stent overlap cannot always be avoided, improved deployment strategies or stent designs could reduce the low WSS burden.

1. Introduction

About 30% of patients undergoing percutaneous coronary intervention (PCI) with stent placement are treated with overlapping stents (Holmes et al., 2004; Räber et al., 2010). Stent overlap is associated with increased risk of adverse clinical outcome for both bare metal stents (BMS) and drug eluting stents (DES) (Ellis et al., 1992; Räber et al., 2010). Various studies have investigated clinical results and biological aspects of stent overlap, but the hemodynamics inside arteries with overlapping stents and the associated wall shear stress (WSS) parameters have received much less attention (Balakrishnan et al., 2005; Charonko et al., 2010; Peacock et al., 1995). This can be in part attributed to the lack of suitable methods for acquiring the geometry of arteries containing overlapping stents with sufficient accuracy.

Stent overlap is associated with increased in-stent restenosis and lumen loss due to delayed healing and increased inflammation regardless of stent type (Räber et al., 2010; Wang et al., 2000). While DES may reduce neointimal hyperplasia and restenosis in single stent cases (Moses et al., 2003; Tsagalou et al., 2005), their performance (Finn et al., 2005; Matsumoto et al., 2007) and safety (Moreno et al., 2005) in regions of overlap are a case of debate. Overlapping BMS are associated with worse clinical outcome compared to single BMS (Kastrati et al., 1999; Kereiakes et al., 2006; Serruys et al., 2002). This is attributed primarily to more pronounced arterial injury caused by the expansion of two stents at the same location, leading to increased inflammation. However, the poorer outcome may also be related to severe hemodynamic disturbances introduced by stent malapposition (Charonko et al., 2010) that are inherent in stent overlap but occur infrequently in single stents (Matsumoto et al., 2007).

It is generally accepted that hemodynamics influences vascular health and pathogenesis. WSS as one of the manifestations of blood flow has been shown to be an important factor in athergenesis (Chatzizisis et al., 2007; Cheng et al., 2006) and in the pathobiology of neointimal hyperplasia, thrombosis and in-stent restenosis (Papafaklis et al., 2010; Wentzel et al., 2008). These latter processes are a concern in percutaneous vascular intervention in general and in stent placement in particular. For example, stent malapposition has been shown to increase thrombogenicity. It is hypothesized that hemodynamics plays a role therein, as

* Corresponding author at: The Interface Group, Institute of Physiology, University of Zurich, Winterthurerstrasse 190, Y23 J8, 8057 Zurich, Switzerland. Tel.: +41 44 635 50 55; fax: +41 44 635 68 14.
E-mail address: vartan.kurtcuoglu@uzh.ch (V. Kurtcuoglu).

0021-9290/$ - see front matter © 2013 Elsevier Ltd. All rights reserved.
http://dx.doi.org/10.1016/j.jbiomech.2013.10.048

adjacent high shear stress areas and recirculation zones caused by malapposed stents may activate platelets and increase local residence times of these thrombocytes (Hathcock, 2006; Kolandaivelu et al., 2011; Peacock et al., 1995). Kolandaivelu and co-workers showed in vitro and in a 2D computational model with idealized domain geometry that flow recirculation between malapposed and overlapping stent struts may modulate stent thrombogenicity (Kolandaivelu et al., 2011).

Computational fluid dynamics (CFD) is the method of choice for assessing shear stress and local hemodynamics in stented arteries. The precise acquisition of the stent struts and arterial geometry is a prerequisite for accurate CFD analysis, but no clinical imaging modality exists that could yield such data with sufficient resolution. Several approaches have been reported in the literature to circumvent this limitation: simulations may be conducted on idealized geometries based on stent CAD data (Gundert et al., 2011), on hybrid domains where the stent free geometry is obtained by CT, digital angiography or MRI and a stent is virtually implanted (De Santis et al., 2010; LaDisa et al., 2006), on ex vivo micro-computed tomography (μCT) data of explanted, stented arteries (Morlacchi et al., 2011) or μCT images of stented in vitro artery models (Benndorf et al., 2009; Connolley et al., 2007). While these methods have their undisputed respective strengths, they have either limited geometric accuracy, limited treatable vascular domain size or incomplete representation of the mechanical interaction between stent and arterial wall.

We have recently introduced a method that allows for precise ex vivo acquisition of arteries stented in vivo or ex vivo, yielding both the macroscopic arterial tree geometry as well as the configuration and morphology of individual stent struts (Rikhtegar et al., 2013). Here we make use of this method to investigate the shear stress distribution and hemodynamics of porcine coronary arteries with overlapping stents. Our goal is to evaluate flow disturbances and consequent shear stress alterations introduced by stent overlap which may contribute to the reported clinical problems associated with overlapping stents.

2. Methods

A concise description of the utilized methods is given here. We refer the reader to the Supplemental material and Rikhtegar et al. (2013) for a more detailed explanation of the individual process steps.

2.1. Heart preparation, stenting and vascular corrosion casting

After cannulation, two absorbable metal scaffolds of 10 mm length and 3 mm diameter (Biotronik AG, Switzerland) were implanted in the left coronary artery of 11 ex vivo porcine hearts under angiographic guidance by an interventional cardiologist. The scaffolds had overlap in 6 arteries. The remaining 5 arteries served as control (no overlap).

A radio-opaque casting material was prepared as a mixture of Biodur E20 resin (Biodur Products GmbH, Germany) and iodine-saturated methyl ethyl ketone solvent. The casting material was injected into the stented arteries under physiological pressure of 90 mm Hg. The hearts were left at room temperature for 36 h, and then macerated at 55 °C in a 7.5% w/v solution of potassium hydroxide. The final products were rinsed with water to remove remaining tissue.

2.2. μCT imaging of stented casts and image processing

Micro-computed tomography (μCT80, Scanco Medical AG, Switzerland) was used with an isotropic voxel size of 74 μm (energy 70 kVp, integration time 300 ms, tube current 114 μA, and two times frame averaging) to capture the overall geometry of the arterial tree. The stented vessel segments were dissected from the remainder of the arterial tree and re-scanned at higher resolution (μCT40, Scanco) with an isotropic voxel size of 6 μm (energy 70 kVp, integration time 300 ms, tube current 114 μA, and two times frame averaging).

To partly suppress noise in the raw μCT volumes, a constrained 3D Gauss filter was used ($\sigma = 1.2$ and support$=1$). Both μCT datasets of low and high resolution were independently segmented using a semi-automatic, intensity-based approach in Avizo 6.2 (Visualization Sciences Group SAS, France) to obtain the lumen geometry. The resulting 3D geometries were exported to Geomagic Studio 12 (Geomagic, Inc., USA) to register and merge the high resolution geometry of the stented segment and the low resolution remainder of the arterial tree.

2.3. CFD calculations

ANSYS ICEM CFD (ANSYS, Inc., USA) was used to generate a computational grid consisting of approximately 50 million tetrahedral elements in the merged geometry. Steady-state CFD analysis was carried out with the finite volume code ANSYS CFX to determine hemodynamics and WSS distribution. Blood was modeled as a non-Newtonian fluid with constant density of 1050 kg/m^3 and shear dependent dynamic viscosity according to the Carreau model (Chien et al., 1966). Inflow rate was set to 0.95 mL/s at the coronary ostium (Berne and Levy, 1986) and no slip was prescribed at the stent surfaces and vessel wall. Murray's law was applied at the outlets to where the largest diameter branch had zero relative pressure. Outflow rates at the remaining outlets were determined according to their cross-sectional area (Murray, 1926; Rikhtegar et al., 2013). Residual reduction to 10^{-8} of the initial value was set as the convergence criterion. Grid independence studies confirmed that the chosen grid was sufficient to capture WSS with a relative error of $< 4\%$ compared to a grid with 100% higher cell density.

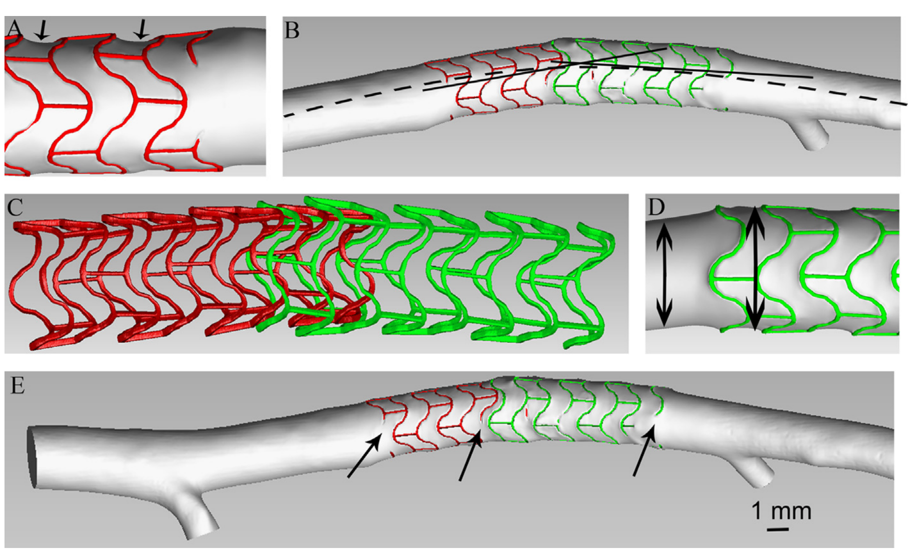

Fig. 1. Porcine left coronary artery lumen negative with two overlapping stents. (A) Areas of tissue prolapse (arrows) between stent struts (red). (B) Axial arterial deformation due to stenting. The solid lines show the individual longitudinal axes of the two deployed stents (red and green), while the dashed line approximates the centerline of the stent-free artery. (C) Reconstructed surface of overlapping stents, visualizing relative strut positioning in the region of overlap. (D) Radial arterial deformation caused by stenting. The arrows indicate arterial diameter in the stented (right) and stent-free regions. (E) The embedded stents with the captured lumen negative. Malapposed strut sections are marked by arrows. (For interpretation of the references to color in this figure legend, the reader is referred to the web version of this article).